

Lab on a Chip

Accepted Manuscript



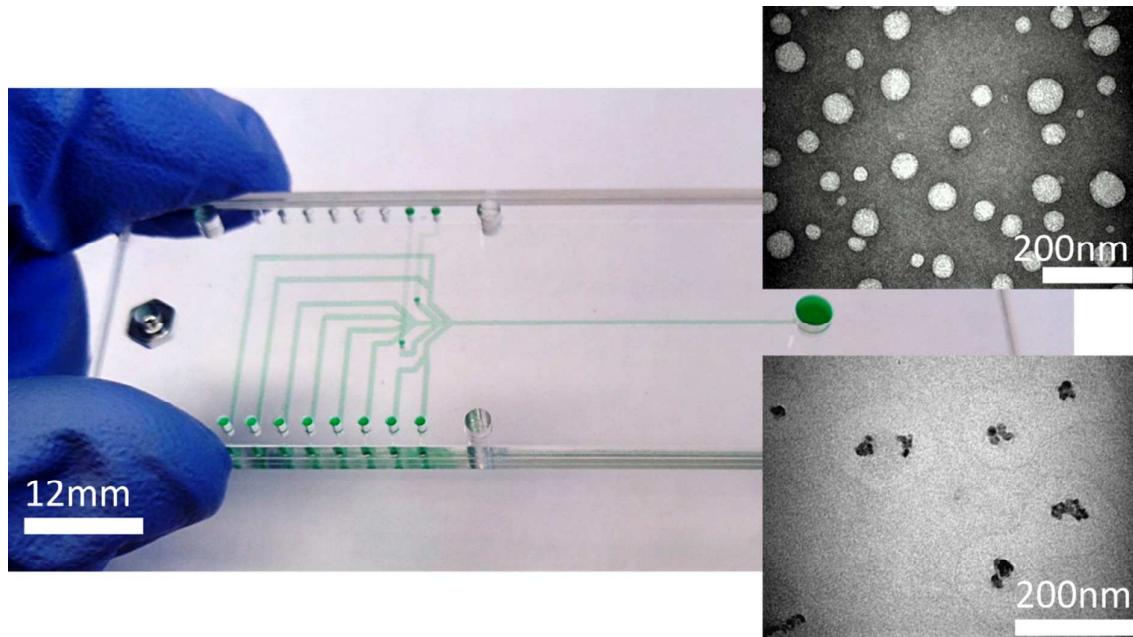
This is an *Accepted Manuscript*, which has been through the Royal Society of Chemistry peer review process and has been accepted for publication.

Accepted Manuscripts are published online shortly after acceptance, before technical editing, formatting and proof reading. Using this free service, authors can make their results available to the community, in citable form, before we publish the edited article. We will replace this *Accepted Manuscript* with the edited and formatted *Advance Article* as soon as it is available.

You can find more information about *Accepted Manuscripts* in the [Information for Authors](#).

Please note that technical editing may introduce minor changes to the text and/or graphics, which may alter content. The journal's standard [Terms & Conditions](#) and the [Ethical guidelines](#) still apply. In no event shall the Royal Society of Chemistry be held responsible for any errors or omissions in this *Accepted Manuscript* or any consequences arising from the use of any information it contains.

A low-cost, portable microfluidic platform for preparing monodisperse magnetoliposomal suspensions that does not require extrusion steps.



Continuous flow generation of magnetoliposomes in a low-cost portable microfluidic platform

Cite this: DOI: 10.1039/x0xx00000x

Received 00th January 2014,
Accepted 00th January 2014

DOI: 10.1039/x0xx00000x

www.rsc.org/

Alvaro J. Conde^{a*†}, Milena Batalla^{b*}, Belén Cerda^b, Olga Mykhaylyk^c, Christian Plank^c, Osvaldo Podhajcer^d, Juan M. Cabaleiro^e, Rossana E. Madrid^a and Lucia Policastro^{b†}

We present a low-cost, portable microfluidic platform that uses laminated poly-methylmethacrylate chips, peristaltic micropumps and LEGO® Mindstorms components for the generation of magnetoliposomes that does not require extrusion steps. Combinations of lipids reconstituted in ethanol and an aqueous phase were injected independently in order to generate a combination of laminar flows in such a way that we could effectively achieve four hydrodynamic focused nanovesicle-generation streams. Monodisperse magnetoliposomes with characteristics comparable to those obtained by traditional methods have been obtained. The magnetoliposomes are responsive to external magnetic field gradients, result that suggests that the nanovesicles can be used in research and applications of nanomedicine.

Introduction

Liposomes containing magnetic nanoparticles or magnetoliposomes (MLs) have been studied extensively because their magnetic nature allows them to concentrate therapeutic drugs at specific sites through the application of permanent gradient magnetic fields, without the use of molecular-targeting agents.^{1,2} They can also be used in combination with hyperthermia cancer treatment due to the heat-generating properties of magnetic nanoparticles (MNPs) when exposed to an alternating magnetic field. Moreover, MNPs entrapped within the lipid bilayer or in the core of thermosensitive MLs are able to act as heat mediators promoting the breakdown of the lipid bilayer.^{3,4} In addition, MLs are also useful as contrast agents for magnetic resonance imaging studies and positron emission tomography.^{5,6} MLs can be generated by thin-film hydration, reverse phase evaporation and double emulsion techniques.⁷ These methods often require long post-processing through expensive and bulky equipment to yield an adequate homogeneity, optimal lamellarity and achieve high drug encapsulation rate. Furthermore, traditional methods also require considerable amounts of reagents making the research with liposomes a costly and laborious venture.

Microfluidics is the study of the fluid flows at microscopic scales and it enables precise and predictable fluid control because of the laminar regime - due to very low Reynolds number - in which these systems usually operate.⁸ Novel

microfluidic-based techniques have been investigated to produce liposomes in the last years. These new technologies offer a range of advantages compared to conventional bulk methods, for instance improved process control and reproducibility accompanied by features such as very good uniformity of nanomaterial characteristics and efficient use of materials and reagents.⁹ Reviews illustrating the advantages and constrains of different microfluidic techniques for liposome production have been recently published.^{10,11} Among these, the hydrodynamic focusing technique has drawn special attention since its introduction by Jahn *et al.*¹² The process involves a stream of lipids dissolved in an organic solvent passing between two aqueous streams in a microfluidic channel. The liposomes are formed by a diffusively driven process at the liquid interfaces. Yield, size and encapsulation efficiency of the nanovesicles can be controlled by modulating the flow rate ratio between the aqueous and organic solvent streams. In this way, post-processing steps (inherent to traditional methods) - especially size reduction by extrusion - can be avoided saving considerable time and reagents.¹³ Moreover, this technique can be used for high-throughput vesicle production.¹⁴

Seth *et al.* have explored the encapsulation of magnetic nanoparticles in liposomes by the microfluidic double emulsion technique, but this method produces giant vesicles that are not always suitable for systemic therapeutic application.¹⁵ To the best of our knowledge, there is no peer-reviewed published

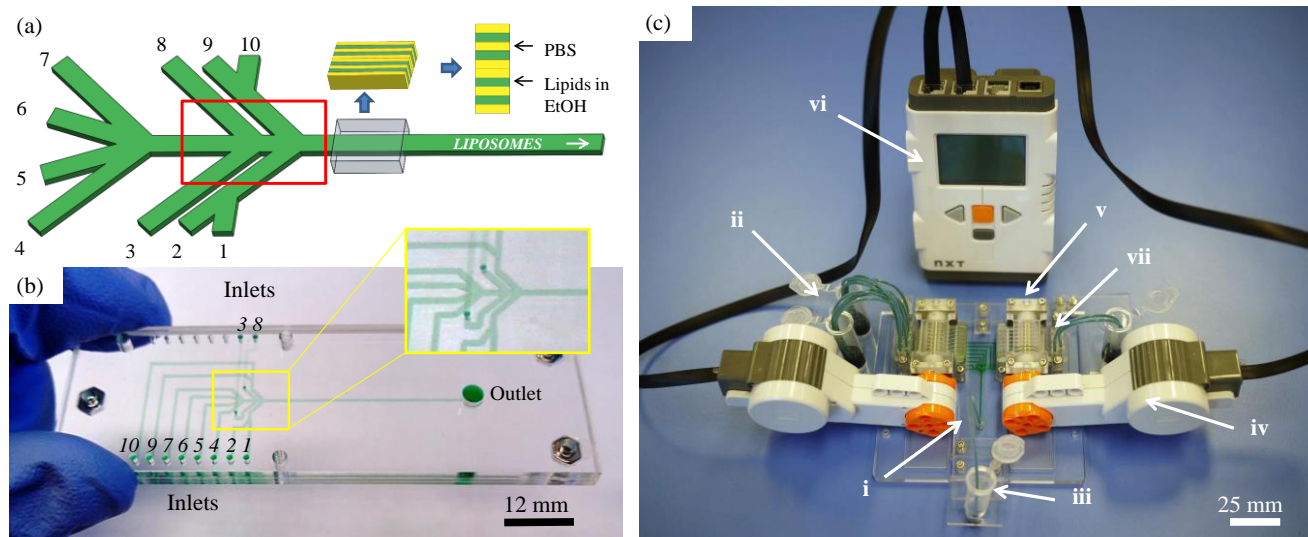


Fig. 1 (a) 10-inlet microfluidic configuration. Aqueous phase (PBS) contains the hydrophilic substance/particle of interest to be encapsulated within liposomes (inputs 1, 3, 5, 6, 8 and 10). Inputs 2, 4, 7 and 9 contain the lipids dissolved in organic phase (ethanol). The yellow and green stripes illustrate how the final distribution of PBS and lipids in EtOH within the channel will be. (b) Fabricated PMMA chip filled with green food dye for easier visualization of the channels. (c) Microfluidic platform for liposome generation: i- microfluidic chip, ii- inlet vials, iii-outlet vial, iv- LEGO® servomotors, v- peristaltic micropump, vi- LEGO® control brick and vii- inlet connector.

work investigating the generation of magnetoliposomes *via* microfluidic hydrodynamic focusing.

Here we present a continuous flow magnetoliposome generation system *via* 2D microfluidic hydrodynamic focusing based on a microfluidic platform developed by Sabourin *et al.*, the MainSTREAM component platform.¹⁶ The complete system is small, simple and cheap but still gives high quality results: the fabricated nanovesicles are monodisperse and similar to those obtained by traditional methods. They are also responsive to external magnetic field gradients. These results suggest that they might be good candidates for nanomedicine research and applications. Also we demonstrate the feasibility of a peristaltic micropump for performing hydrodynamic focusing for this kind of processes.

Materials and methods

Microfluidic chip and platform

We first investigated a 6-inlet configuration (Fig. S1) with a single flow focusing zone, *i.e.*, an ethanol phase focused by two phosphate buffer saline (PBS) phases, following what most authors have done so far, but the obtained liposomes and magnetoliposomes size distributions were not homogeneous nor adequate for potential *in-vitro* or *in-vivo* assays so we proposed a different configuration.^{12,13, 17-19} Koh *et al.* investigated a 5-inlet design - with 2 hydrodynamic flow focusing zones - where they address a similar size and homogeneity problem.²⁰ Due to channel availability in the peristaltic micropump - 8 channels per pump - a 10-inlet microfluidic configuration, shown in Fig. 1a, was used for magnetoliposomes generation in this work. It is important to highlight that this configuration has four hydrodynamic flow focusing zones.

Aqueous phase (PBS) containing or not the hydrophilic substance/particle of interest to be encapsulated flows in

channels 1, 3, 5, 6, 8 and 10 and lipids dissolved in ethanol phase flows in channels 2, 4, 7 and 9. The flow rate ratio (FRR) is defined as the ratio of aqueous phase volumetric flow rate (VFR), Q_{PBS} , to lipids dissolved in ethanol VFR, Q_L .

Microfluidic chips were fabricated by computer numerical control (CNC) micromilling in accordance to a previously published work.²¹ The chips consist of three layers made from 1 mm thick optical quality poly-methylmetacrylate (PMMA) sheets (Clarex, Japan). The channels width and depth were 400 μm and 150 μm respectively. These parameters can be easily changed by using different end mills and setting different depths in the computer-aided manufacturing (CAM) process. The hydrodynamic focusing channel length is 30 mm. In order to obtain closed channels, the chip slides were bonded *via* a thermal UV-assisted bonding process.²² Previously, the chip slides were gently cleaned to remove debris, sonicated in isopropyl alcohol for 2 min, rinsed with deionized water and finally blown dry with filtered air. Bonding faces of the microfluidic chips were exposed to UV (250 W quartz mercury lamp) for 1 min and subsequently bonded between glass plates in a bonding press (Shimeq, Argentina) at 80 °C for 15 min with an applied pressure of 2 MPa. A photo of a finished chip can be seen in Fig. 1b. More information about chip fabrication can be found in the supplementary information (Fig. S2).

Pumping was done by two 8-channel peristaltic micropumps that have been previously described.¹⁶ Each micropump is driven by a LEGO® Mindstorms NXT 2.0 servomotor and controlled by the LEGO® Mindstorms NXT 2.0 brick. The micropumps were connected directly to the chip and to a custom made inlet connector *via* polydimethylsiloxane (PDMS) microfluidic ribbons.¹⁶ Polytetrafluoroethylene (PTFE) tubing, ID: 0.8 mm/OD: 1.6 mm (Bola Bohlender, Germany), are inserted to each port of the inlet connector shrouded with 4 mm long pieces of silicone tubing, ID: 1

mm/OD: 3 mm, in order to have a liquid-tight connection. The PTFE tubing are connected to its corresponding microcentrifuge tube (Eppendorf, Germany) containing the components needed for the liposome generation. The single outlet of the microfluidic chip is connected directly to a PTFE tube (also shrouded with a piece of silicone) that ends in a collection microcentrifuge tube. A custom-made base plate to fit the two pumps, the microfluidic chip and the LEGO® servomotors was CNC-milled from a 5 mm thick PMMA sheet. The base plate can also hold the inlet and outlet vials. The complete microfluidic system is shown in Fig. 1c.

Numerical simulation

Laminar flow, complete miscibility and small viscosity differences (only 20% at 20 °C) between ethanol and PBS enables predictable microfluidic mixing in our system allowing for numerical analysis of the problem.¹⁹ Direct numerical simulations of the concentration distributions of injected PBS and ethanol streams have been carried out. A finite volumes code developed by Electricité de France (EDF), called Code Saturne, was used to run 2D and 3D time-dependent and steady state simulations.²³ Since the microfluidic configuration is symmetric, only half of the channels geometry is solved and then mirrored for visualization and analysis. We used a 99200 volumes structured mesh for the 2D cases and a 2083200 volumes structured mesh for the 3D cases. Both of the meshes were refined near the walls and corners. Full Navier Stokes equations for incompressible flow coupled to the convection diffusion equation were solved. Viscosity was held constant. However, in future studies, a simulation taking into account the variation of viscosity as a function of ethanol concentration is possible.

Experimentally obtained instantaneous flow rate of the peristaltic micropump (data not shown) running at 25 $\mu\text{l}/\text{min}$ was interpolated and then loaded in Code Saturne as an input for each channel. Steady state flow of 25 $\mu\text{l}/\text{min}$ was also simulated in order to compare with syringe pump setups.

Magnetoliposome preparation

The whole magnetoliposome preparation procedure was performed under sterile conditions inside a biological safety cabinet. Once the microfluidic system is fully assembled, a 0.5 M solution of NaOH in water is flushed through all the channels at 10 $\mu\text{l}/\text{min}$ for 30 min for complete sterilization of the tubing and the microfluidic channels of the chip.²⁴ After sterilization, sterilized MiliQ water is flushed through all the channels at 10 $\mu\text{l}/\text{min}$ for 30 min for complete base removal of the system. Sterile microcentrifuge tubes and pipette tips are used at all time.

A combination of 93:3:4 molar ratio of 1-palmitoyl-2-oleoyl-sn-glycero-3-phosphocholine (POPC), dimethyldioctadecylammonium bromide (DDAB) and phosphoethanolamine-[methoxy(polyethyleneglycol)-2000] (PEG2000-DSPE) (all from Avanti Polar Lipids Inc., Alabaster, AL) was dissolved in chloroform (Mallinckrodt Baker, Inc.,

Paris, KY) and placed under nitrogen stream for complete solvent evaporation for 8 hours. The lipid film was then reconstituted in ethanol 90% (Sigma-Aldrich, St. Louis, MO) for a total lipid concentration of 40 mM. Magnetoliposomes were generated by injecting 0.5 ml of the ethanol reconstituted lipids mixture and 0.5 ml of SO-Mag5 magnetic nanoparticle suspension (5 mg Fe/ml) in PBS through the mentioned channels shown in Fig. 1a. Core-shell type SO-Mag5 were stabilized by a silicon oxide layer with surface phosphonate groups; yielding a negative ζ potential of -38 ± 2 mV, and had a mean hydrodynamic diameter of 40 nm when measured in aqueous suspension. The dry nanomaterial contained 0.52 g of iron per gram of total weight; they were synthesized according to the reported method.²⁵ Non-magnetic liposomes were generated using the same methodology but injecting only PBS through the corresponding microchannels.

Ethanol reconstituted lipids VFR (Q_L) and PBS VFR (Q_{PBS}) were set to 25 $\mu\text{l}/\text{min}$ in all channels. These values yield a total $Q_{PBS} = 150$ $\mu\text{l}/\text{min}$ and a total $Q_L = 100$ $\mu\text{l}/\text{min}$ respectively resulting in a FRR of 15:10 (or 1.5:1) and a total volumetric flow rate of 250 $\mu\text{l}/\text{min}$. Ethanol concentration was 90% v/v which can be seen as a flow rate of 90 $\mu\text{l}/\text{min}$ of 100% v/v ethanol, that in a total flow rate of 250 $\mu\text{l}/\text{min}$ yields a final ethanol concentration of 36%. Empty liposomes and magnetoliposomes were sonicated for 0.5 min and dialyzed against HBS 20 mM pH 7 overnight. Before dialysis, magnetoliposome suspension was centrifuged at 1000 g for 15 min in order to remove unencapsulated magnetic nanoparticles.²⁶

For the sake of comparison, we additionally produced magnetoliposomes by the film hydration method. Briefly, 20 μmoles of total lipid (POPC:DDAB:DSPE-PEG-2000 = 93:3:4 molar ratio) were dissolved in chloroform and evaporated using nitrogen stream. The lipid film was then hydrated in 1 ml of 2.5 mg Fe/ml of MNPs suspension in order to maintain the 1:5 Fe/lipid w/w ratio. The preparation was subsequently extruded through 800 nm, 400 nm and 200 nm polycarbonate membranes using an extruder (Avanti Polar Lipids, USA). Finally, the liposomes were sonicated for 0.5 min and centrifuged at 1000 g for 15 min in order to remove unencapsulated magnetic nanoparticles.

Magnetoliposome characterization

Mean size distribution and polydispersity index (PI) of empty liposomes and magnetoliposomes were determined by dynamic light scattering (Zetasizer Nano; Malvern, UK). Morphological aspects were observed by transmission electron microscopy according to the reported methods.²⁷ Drops of magnetoliposomes samples were placed over 200 mesh copper grids coated with carbon film and excess liquid was removed by blotting with filter paper. Negative staining was performed using 2% uranyl acetate.²⁶ The samples were then observed in a Philips CM200 (Philips, Netherlands) transmission electron microscope with EDAX microanalysis and 160 kV of accelerating voltage. Magnetic nanoparticles encapsulation

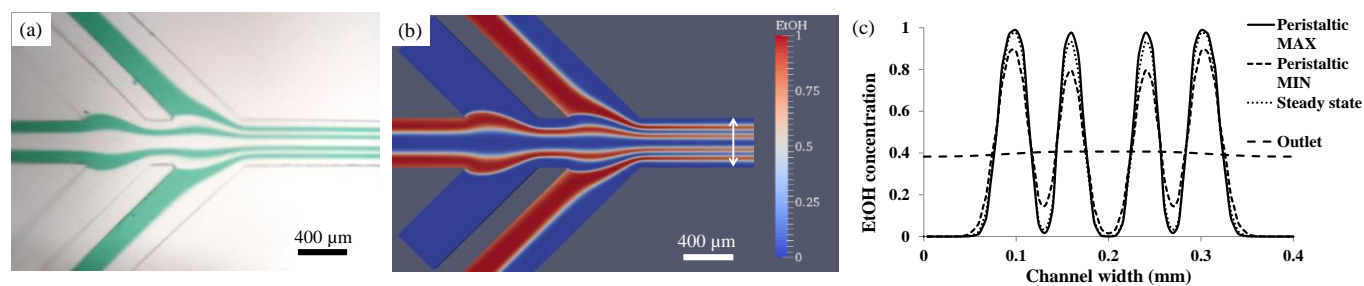


Fig. 2 (a) Micrograph of the area highlighted inside the red square in Fig. 1a running green food dye and water, (b) XY vertical midplane slice of the 3D finite element method simulation of the same area shown in Fig. 2a and (c) plot over line (white double arrow in Fig. 2b) of the ethanol relative concentration distribution profiles for peristaltic flow and steady state. Outlet plot in Fig. 2c represents CDP at the end of the channel (30 mm distance from final merging point) and demonstrates the mixing effect at the exit of the microfluidic chip for a steady state situation.

efficiency of the liposomes was evaluated as the iron/phospholipid w/w ratio.²⁷ Iron concentration was determined spectrophotometrically at 508 nm by complexation with 1,10-phenanthroline.²⁸ Phospholipids were previously extracted by Bligh & Dyer method and quantified by Bartlett-modified method.²⁷

Magnetic responsiveness of magnetoliposomes

In order to evaluate the magnetic responsiveness (or magnetophoretic mobility) we calculated the average velocity of magnetoliposomes exposed to a defined magnetic field. A suspension of MLs contained in an optical cuvette was exposed between two sets of 4 quadrangular Ne-Fe-B permanent magnets (18x16x4 mm) and optical density (or turbidity) at 360 nm was measured during 30 min. The average velocity v (m/s) under a magnetic field gradient is evaluated as

$$v = L/t_{0.1} \quad (1)$$

where L (m) is the average path of the complex movement perpendicular to the measuring light beam and $t_{0.1}$ is the time required for a ten-fold decrease in optical density. Further calculation of the average magnetic moment M (A·m²) of the magnetoliposome and estimation of the number of magnetic nanoparticles associated with the liposomes was performed taking into account the hydrodynamic diameter, core size of the complexes and magnetization of the nanoparticles as described by Wilhelm *et al.*²⁹

Results and discussion

Hydrodynamic flow focusing with a peristaltic micropump

The Reynolds number in the hydrodynamic flow focusing region of this system can be approximated as

$$Re = QD_H/\nu A \quad (2)$$

where Q is the volumetric flow rate (m³/s), D_H is the hydraulic diameter of the microchannel (m), ν the kinematic viscosity (m²/s) and A is the microchannel cross-sectional area (m²). From eqn (2) we obtained a $Re=14$ considering the kinematic viscosity of water as the worst case scenario, value that corroborates we are working in a laminar regime. Fig. 2a shows

a micrograph of the microfluidic system running green food dye and water at 25 μ l/min in all channels. This figure corresponds to the highlighted area inside the red square in Fig. 1a and was intended for a clear visualization of the different streams inside the microfluidic channel. This photograph clearly corresponds very well with the 3D numerical simulation (XY vertical midplane slice) of the system presented in Fig. 2b.

It is important to note that the peristaltic flow is a time-dependent flow and the micrograph and simulation shown in Fig. 2a and Fig. 2b respectively are snapshots that were taken in a specific time when the concentration distribution profile (CDP) is similar to that of steady state. In order to compare the different CDPs at different times we plot in Fig. 2c the ethanol (EtOH) concentration in a line across the main channel at a position of 800 μ m from the final merging point when the CDPs are maximum and minimum. It can be seen that they do not differ much from steady state flow but this peristaltic motion perpendicular to the direction of the flow could induce some mixing. A certain amount of mixing (compared to a steady flow state) due to peristaltic flow has been previously observed in a similar system.³⁰ It was later confirmed and quantified by Truesdell *et al.* where they stated that mixing of peristaltic flows can be a 31% better than steady state flows.³¹ However this percentage can only be achieved at very long distances from the merging point (of the streams that are to be mixed) and care must be taken to ensure that the inlet flows are in full contra-phase. Pumping in our system is done in-phase but inherent microfabrication differences can result in average displaced flows with a 6% difference from each other even within the same pump, so for experimental purposes we can consider that our flows are slightly out of phase.¹⁶ Truesdell *et al.* state that for this kind of peristaltic flow, folds can be observed at 82 diameters long, which in our system yields a distance of 32 mm, 2 mm longer than the main channel. However this value is close to the fall within the system and to verify that diffusion alone will mix the sample before any mixing originating from peristaltic flow, we simulated the complete system in 2D with the full length of the channel, *i.e.*, 30 mm, in a steady state flow condition. In this simulation we plotted the CDPs at a distance of 30 mm and it is shown in Fig. 2c as the middle line, tagged as “outlet” in the legend. From this information it can be seen that mixing is almost complete at

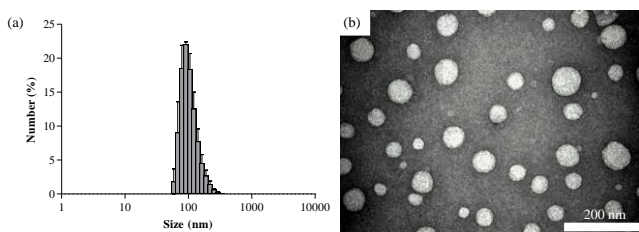


Fig. 3 (a) DLS number size distribution of the empty liposomes generated by the microfluidic hydrodynamic focusing method. (b) TEM images of the empty liposomes stained with uranyl acetate 2%.

this distance. Experimental results, shown in Fig. S3, further demonstrate that mixing is close to full development at the end of the focusing channel. From these results we can conclude that peristaltic mixing in our system can be neglected and CDPs would be similar to steady state flow condition, *i.e.*, the flow that would be obtained with syringe pumps.

The MainSTREAM platform overcomes the key problem related to liposome generation in microfluidic systems: the use of expensive and bulky syringe pumps, which usually result in small microfluidic chips that need to be connected to actuators and reservoirs through long tubing which yields large dead volumes, poor liquid control (due to pressure buildups) and limits system portability.¹⁶ The MainSTREAM platform minimizes all these aspects: it uses short tubing with minimum dead volumes, small multichannel micropumps and more convenient microfluidic chips that are easier to handle, mount and fit tubing/connectors. Moreover microchannels in this size range are easier to fabricate, operate and do not clog so easily as smaller ones.¹⁹ The manufacturing cost of all the MainSTREAM platform components and LEGO® modules does not exceed a few hundred dollars; value that is negligible when compared to the cost of a single precision syringe pump that it is approximately 10 times higher.¹⁶ Additionally, the complete set-up used in this work needs no more components than shown in Fig. 1c, making platform's footprint small when compared to syringe pumps set ups enabling system portability.

Magnetoliposome generation

In order to test the performance of the microfluidic system we first generated empty liposomes. The mean size was 90 ± 28 nm with a polydispersity index of 0.165 (Fig. 3a). TEM images showed typical spherical morphology and good size uniformity (Fig. 3b).

Magnetic nanoparticles and magnetoliposomes number size distributions are shown in Fig. 4a and Fig. 4b respectively. The mean sizes of the MNPs and MLs were 68 ± 11 nm (PI 0.188) and 158 ± 30 nm (PI 0.180) respectively ($n=3$). The intensity distribution of MLs sizes (Fig. S4) shows that about 70% of population has a diameter between 90-220 nm, demonstrating that the MLs are the main component. The size and PI indicate that these magnetoliposomes could be adequate for *in-vitro* or *in-vivo* applications.

MLs and MNPs morphologies were observed through transmission electronic microscopy and are presented in Fig. 4 b, c, d and e. MNPs were observed in higher extent inside of the

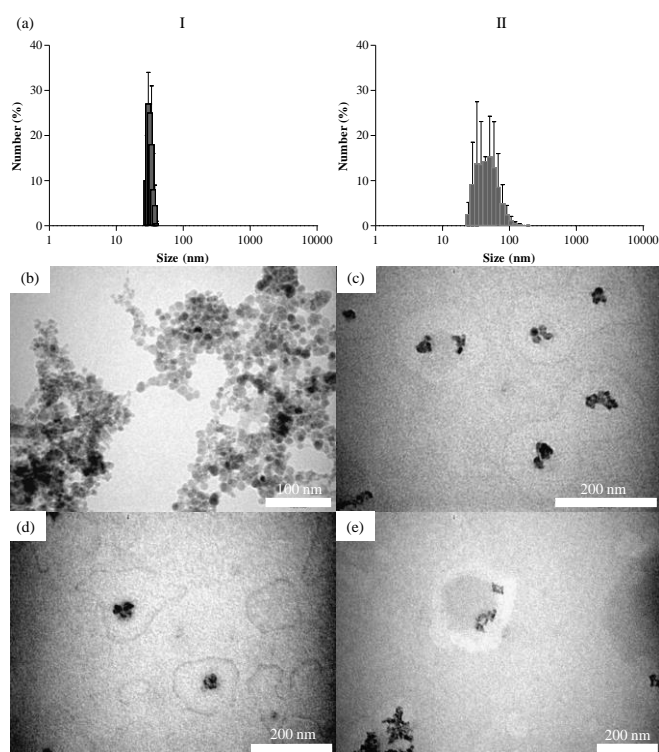


Fig. 4 (a) DLS number size distributions of the (I) magnetic nanoparticles SO-Mag5 and (II) magnetoliposomes obtained by microfluidic hydrodynamic focusing method. TEM images of: (b) magnetic nanoparticles SO-Mag5; (c)-(d)-(e) magnetic-responsive magnetoliposomes obtained by microfluidic hydrodynamic focusing method stained with uranyl acetate 2%.

liposomes (Fig. 4c) although some MNPs were also present on the lipid surface (Fig. 4e). The size and morphology of the liposomes were preserved with almost no alteration for at least one month after its generation (data not shown).

The iron/phospholipid (Fe/PL) molar ratio of MLs was 4.1 ± 1.1 Fe/PL.

Magnetoliposomes obtained by traditional methods (film hydration) have shown similar sizes (145 ± 35 ; PI 0.17) and similar iron/phospholipid molar ratio (4.1 ± 1.8 Fe/PL).

Magnetic responsiveness of magnetoliposomes

The time course of the normalized turbidity of magnetoliposomes suspension is plotted in Fig. 5.

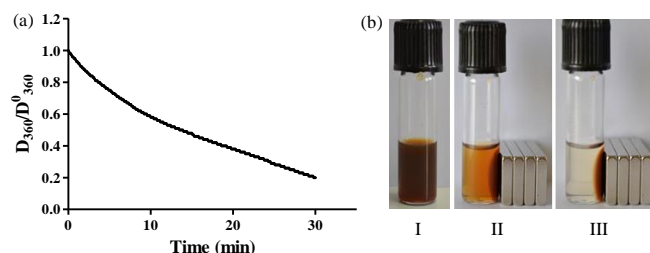


Fig. 5 (a) Time course of the normalized turbidity of the magnetoliposomal suspension upon application of the gradient magnetic field (average field and field gradient of 213 mT and 4 Tm^{-1}). (b) Photographs of MLs suspension without magnetic field (I), and upon application of the gradient magnetic field for minutes (II) and hours (III).

The experimental data were fitted to an exponential decay equation and it was calculated that 90% of the magnetoliposomes are sedimented within 43 min after the magnetic field was applied. Replacing these values in eqn (1) yields a magnetophoretic mobility of 0.35 $\mu\text{m/s}$. Considering this value and the average hydrodynamic diameter of the vesicles of 158 ± 30 nm, yields an estimated average magnetic moment of $2.7 \cdot 10^{-16}$ A·m². These results confirm that the obtained nanovesicles are in fact responsive to external magnetic fields and could be used in the same biomedicine and biological applications as the magnetoliposomes produced by traditional methods.

Conclusions

The magnetoliposomes were generated by four 2D hydrodynamic flow focusing zones in a low-cost, portable microfluidic system based on the MainSTREAM component platform. The morphology, size and magnetic responsiveness of the nanovesicles were measured and verified to be similar to those of magnetoliposomes obtained by traditional methods.

The system was also validated for the generation of empty liposomes and results were also found to be similar to those obtained with traditional methods. The suitability of a peristaltic micropump for performing hydrodynamic focusing for nanovesicle-generation was evaluated by numerical simulations and experimental analyses and found to be adequate for these kinds of processes under certain conditions.

The low-cost and portability features of the developed microfluidic system could allow for implementation of personalized and/or point-of-care production of nanomedicine, reducing limitations and costs associated with most of the traditional liposomal preparations.

Acknowledgments

This work was partially supported by grants and/or funds from the Agencia Nacional de Promoción Científica y Tecnológica, Consejo Nacional de Investigaciones Científicas y Técnicas, Comisión Nacional de Energía Atómica (CNEA), Instituto Superior de Investigaciones Biológicas (INSIBIO) and the Consejo de Investigaciones de la Universidad Nacional de Tucumán (CIUNT).

We specially thank to all members of División Bioquímica Nuclear, División de Olfatometría and Laboratorio de Microscopía and CNEA authorities for invaluable support and assistance at all levels during the last year. We also thank all the members of the Centro de Micro y Nanoelectrónica del Bicentenario (CMNB) of the Instituto Nacional de Tecnología Industrial (INTI) where the microfluidic chips were fabricated.

Notes and References

^a LAMEIN, Departamento de Bioingeniería, Facultad de Ciencias Exactas y Tecnología, Universidad Nacional de Tucumán / Instituto Superior de Investigaciones Biológicas, Consejo Nacional de Investigaciones Científicas y Técnicas (CONICET), Av. Independencia 1800, Tucumán, Argentina. E-mail: aconde@herrera.unt.edu.ar Tel: +54-381-4364120

^b Laboratorio de Nanomedicina, Instituto de Nanociencia y Nanotecnología, Comisión Nacional de Energía Atómica - CONICET, Av. General Paz 1499, Buenos Aires, Argentina. E-mail: policast@cnea.gov.ar Tel.: +54-11-67727000 – Int. 6575. Fax: +54-11-67727134

^c Institute of Experimental Oncology and Therapy Research, Technische Universität München, Ismaninger Str. 22, 81675 Munich, Germany. E-mail: olga.mykhaylyk@lrz.tu-muenchen.de Tel.: +49(0)89-4140-4475. Fax: +49(0)89-4140-4476

^d Laboratorio de Terapia Molecular y Celular, Fundación Instituto Leloir, Av. Patricias Argentinas 435, Buenos Aires, Argentina. E-mail: opodhajcer@leloir.org.ar Tel.: +54-11-52387500 – Int. 2108. Fax: +54-11-2387501

^e Laboratorio de Fluidodinámica, Facultad de Ingeniería, Universidad de Buenos Aires - CONICET, Av. Paseo Colón 850, Buenos Aires, Argentina / Laboratorio de Micro y Nanofluidica y Plasma, Universidad de la Marina Mercante, Av. Rivadavia 2258, Buenos Aires, Argentina. E-mail: jmcabaleiro@fi.uba.ar Tel.: +541143430891 – Int. 1095.

† These authors are co-corresponding authors.

* These authors contributed equally.

- 1 M. R. Mozafari, *Methods Mol. Biol.*, 2010, **605**, 29-50.
- 2 S. Dandamudi and R.B. Campbell, *Biomaterials*, 2007, **28**, 4673-4683.
- 3 L. A. Tai, P. J. Tsai, Y. C. Wang, Y. J. Wang, L.W. Lo and C. S. Yang, *Nanotechnology*, 2009, **20**, 135101.
- 4 P. Kulshrestha, M. Gogoi, D. Bahadur and R. Banerjee, *Colloids Surf. B Biointerfaces*, 2012, **96**, 1-7.
- 5 G. Mikhaylov, U. Mikac, A. A. Magaeva, V. I. Itin, E. P. Naiden, I. Psakhye, L. Babes, T. Reinheckel, C. Peters, R. Zeiser, M. Bogyo, V. Turk, S. G. Psakhye, B. Turk and O. Vasiljeva, *Nat. Nanotechnol.*, 2011, **6**, 594-602.
- 6 N. K. Devaraj, E. J. Keliher, G. M. Thurber, M. Nahrendorf and R. Weissleder, *Bioconjugate Chem.*, 2009, **20**, 397-401.
- 7 M. D. Cuyper and M. Joniau, *Eur. Biophys. J.*, 1988, **15**, 311-319.
- 8 H.A. Stone, A.D. Stroock and A. Ajdari, *Annu. Rev. Fluid Mech.*, 2004, **36**, 381-411.
- 9 S. Krishnadasan, A. Yashina, A.J. deMello and J.C. deMello, *Advances in Chemical Engineering*, ed. J.C. Schouten, **Vol. 38**, Academic Press, Amsterdam, 2010, ch. 4, pp. 195-231.
- 10 D. van Swaay and A. deMello, *Lab Chip*, 2013, **13**, 752-767.
- 11 Y.P. Patil and S. Jadhav, *Chem. Phys. Lipids.*, 2014, **177**, 8-18.
- 12 A. Jahn, W. N. Vreeland, M. Gaitan and L. E. Locascio, *J. Am. Chem. Soc.*, 2004, **126**, 2674-2675.
- 13 A. Jahn, W. N. Vreeland, D. L. DeVoe, L. E. Locascio and M. Gaitan, *Langmuir*, 2007, **23**, 6289-6293
- 14 X. Huang, R. Caddell, B. Yu, S. Xu, B. Theobald, L. J. Lee and R. J. Lee, *Anticancer Res.*, 2010, **30**, 463-466.
- 15 A. Seth, G. Bealle, E. Santanach-Carreras, A. Abou-Hassan and C. Menager, *Adv. Mater.*, 2012, **24**, 3544-3548.
- 16 D. Sabourin, P. Skafte-Pedersen, M. J. S e, M. Hemmingsen, M. Alberti, V. Coman, J. Petersen, J. Emn eus, J. P. Kutter, D. Snakenborg, F. J rgensen, C. Clausen, K. Holmstr m and M. Dufva, *J. Lab. Autom.*, 2013, **18**, 212-228.
- 17 R. R. Hood, C. Shao, D. M. Omiatek, W. N. Vreeland and D. L. DeVoe, *Pharm. Res.*, 2013, **30**, 1597-1607.
- 18 R. Wi, Y. Oh, C. Chae and D. Kim, *Korea-Aust. Rheol. J.*, 2012, **24**, 129-135.

- 19 A. Jahn, S. M. Stavis, J. S. Hong, W. N. Vreeland, D. L. DeVoe and M. Gaitan, *ACS Nano*, 2010, **4**, 2077-2087.
- 20 C. G. Koh, X. Zhang, S. Liu, S. Golan, B. Yua, X. Yang, J. Guan, Y. Jin, Y. Talmon, N. Muthusamy, K. K. Chan, J. C. Byrd, R. J. Lee, G. Marcucci and L. J. Lee, *J. of Control. Release*, 2010, **141**, 62-69.
- 21 P. Skafte-Pedersen, M. Hemmingsen, D. Sabourin, F. S. Blaga, H. Bruus and M. Dufva, *Biomed. Microdevices*, 2012, **14**, 385-99.
- 22 R. Truckenmuller, P. Henzi, D. Herrmann, V. Saile and W. K. Schomburg, *Microsystem Technol.*, 2004, **10**, 372-374.
- 23 F. Archambeau, N. Mehitoua and M. Sakiz, *Int. J. On Finite Volumes*, 2004, **1**, 1-62.
- 24 P. A. Bauman, L. A. Lawrence, L. Biesert, H. Dichtelmüller, F. Fabbriizzi, R. Gajardo, A. Gröner, J. I. Jorquera, C. Kempf, T. R. Kreil, I. von Hoegen, D. Y. Pifat, S. R. Petteway and K. Cai, *Vox Sang.*, 2006, **91**, 34-40.
- 25 O. Mykhaylyk, T. Sobisch, I. Almstatter, Y. S. Antequera, S. Brandt, M. Anton, M. Doblinger, D. Eberbeck, M. Settles, R. Braren, D. Lerche and C. Plank, *Pharm. Res.*, 2012, **29**, 1344-1365.
- 26 P. Pradhan, J. Giri, F. Rieken, C. Koch, O. Mykhaylyk, M. Döblinger, R. Banerjee, D. Bahadur and C. Plank, *J. Control. Release*, 2010, **142**, 108-121.
- 27 O. Mykhaylyk, Y. S. Antequera, D. Vlaskou and C. Plank, *Nat. Protoc.*, **2**, 2007, 2391-2411.
- 28 H. Nobuto, T. Sugita, T. Kubo, S. Shimose, Y. Yasunaga, T. Murakami and M. Ochi, *Int. J. Cancer*, 2004, **109**, 627-635.
- 29 C. Wilhelm, F. Gazeau and J. C. Bacri, *Eur. Biophys. J.*, 2002, **31**, 118-125.
- 30 W. C. Jackson, F. Kuckuck, B. S. Edwards, A. Mammoli, C. M. Gallegos, G. P. Lopez, T. Buranda and L. A. Sklar, *Cytometry*, 2002, **47**, 183-191.
- 31 R. A. Truesdell, P. V. Vorobieff, L. A. Sklar and A. A. Mammoli, *Phys. Rev. E.*, 2003, **67**, 066304.